Sources and Processes Contributing to Nitrogen Deposition: An Adjoint Model Analysis Applied to Biodiversity Hotspots Worldwide
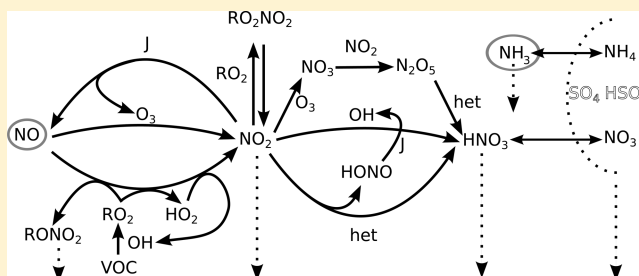
Fabien Paulot,[*,†] Daniel J. Jacob,[†] and Daven K. Henze[‡]

[†]School of Engineering and Applied Sciences, Harvard University, Cambridge, Massachusetts 02138, United States
[‡]Department of Mechanical Engineering, University of Colorado, Boulder, Colorado 80309, United States

S *Supporting Information*

ABSTRACT: Anthropogenic enrichment of reactive nitrogen (Nr) deposition is an ecological concern. We use the adjoint of a global 3-D chemical transport model (GEOS-Chem) to identify the sources and processes that control Nr deposition to an ensemble of biodiversity hotspots worldwide and two U.S. national parks (Cuyahoga and Rocky Mountain). We find that anthropogenic sources dominate deposition at all continental sites and are mainly regional (less than 1000 km) in origin. In Hawaii, Nr supply is controlled by oceanic emissions of ammonia (50%) and anthropogenic sources (50%), with important contributions from Asia and North America. Nr deposition is also sensitive in complicated ways to emissions of SO_2, which affect Nr gas−aerosol partitioning, and of volatile organic compounds (VOCs), which affect oxidant concentrations and produce organic nitrate reservoirs. For example, VOC emissions generally inhibit deposition of locally emitted NO_x but significantly increase Nr deposition downwind. However, in polluted boreal regions, anthropogenic VOC emissions can promote Nr deposition in winter. Uncertainties in chemical rate constants for $OH + NO_2$ and NO_2 hydrolysis also complicate the determination of source−receptor relationships for polluted sites in winter. Application of our adjoint sensitivities to the representative concentration pathways (RCPs) scenarios for 2010−2050 indicates that future decreases in Nr deposition due to NO_x emission controls will be offset by concurrent increases in ammonia emissions from agriculture.

INTRODUCTION

Reactive nitrogen (Nr) deposition has more than tripled since preindustrial times primarily due to Nr production and release from the agriculture and energy sectors.[1] Because Nr is a limiting nutrient in many ecosystems, this increase in Nr deposition has been associated with greater net primary productivity[2−4] but also with threats to biodiversity[5] through pathogens,[6] eutrophication,[7] and loss of species adapted to low Nr availability.[8]

Anthropogenic Nr is released to the atmosphere either as nitrogen oxides ($NO_x \equiv NO + NO_2$), mainly from combustion, or as ammonia (NH_3), mainly from agriculture. NO_x is oxidized in the atmosphere to nitric acid (HNO_3), which is rapidly deposited, and to organic nitrates including peroxyacetylnitrate (PAN), which can serve as reservoirs of Nr and facilitate its long-range transport.[9,10] NH_3 is removed efficiently by wet and dry deposition. NH_3 also partitions into aerosols as ammonium sulfate and ammonium nitrate, which makes it more resistant to dry deposition. In this manner, the long-range transport and deposition of Nr is coupled by atmospheric chemistry to other emissions including volatile organic compounds (VOCs) and sulfur dioxide (SO_2).

The observation network for Nr deposition is sparse and incomplete (e.g, dry deposition is generally not measured). Therefore estimates of Nr deposition generally rely on chemical transport models (CTMs), which relate sources to deposition through atmospheric transport and chemistry and can be evaluated with available observations.[11,12] The processes controlling Nr deposition at a particular receptor site can in principle be fully characterized by perturbing successive source regions, source types, and other processes in the CTM.[12,13] However, this approach is in practice severely limited by the computational expense of conducting a large number of CTM simulations.

The adjoint of a CTM allows the sources and processes controlling Nr deposition at a given receptor site to be characterized more efficiently. Through a single adjoint simulation, we can calculate the model sensitivity of Nr deposition at a particular location to a very large number of model variables for a cost comparable to that of a few forward simulations.[14,15] This technique has been applied previously to characterize source−receptor relationships for NO_x,[16] ozone,[17−21] and black carbon.[22]

Here we use the adjoint of the GEOS-Chem global CTM to determine the sources and other processes contributing to Nr
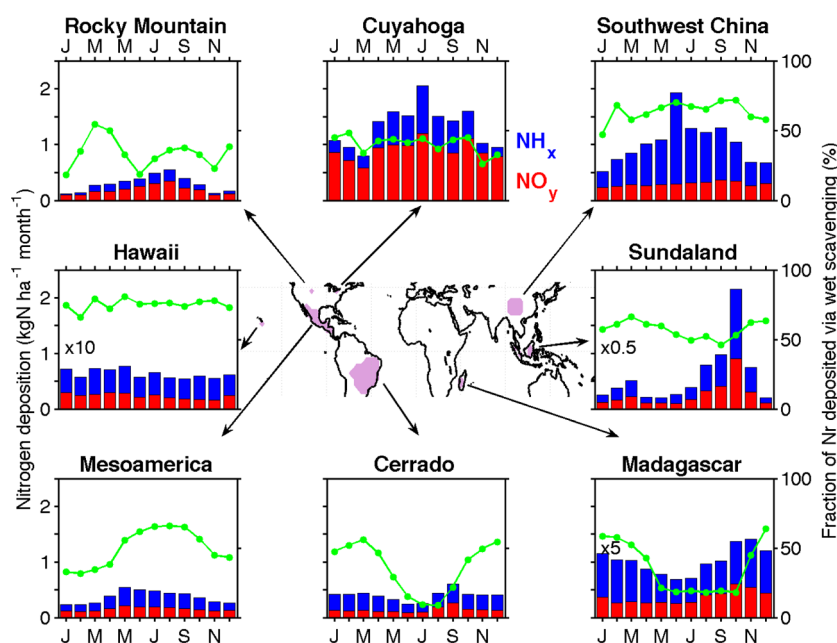
Figure 1. Reactive nitrogen (Nr) deposition in selected biodiversity hotspots and U.S. National Parks (purple) as simulated by GEOS-Chem for 2006. Monthly mean deposition fluxes are shown for reactive nitrogen oxides (NO_y in red) and reduced nitrogen (NH_x in blue). The fraction of Nr removed via wet deposition is shown in green. For Hawaii, Madagascar, and Sundaland, the monthly Nr deposition fluxes have been multiplied by the indicated factor in order to fit on the common scale.

deposition to an ensemble of "biodiversity hotspots" around the world (Figure 1). Biodiversity hotspots are regions that exhibit exceptional richness in flora and fauna but are undergoing major loss of habitat.[23,24] Elevated Nr deposition in these hotspots is of concern.[25] We focus on a representative global subset of biodiversity hotspots: Cerrado (Brazil, 2 000 000 km^2), Madagascar (600 000 km^2), Mesoamerica (central America, 1 100 000 km^2), Volcanoes National Park in Hawaii (1300 km^2), Southwest China (260 000 km^2), and Sundaland (Malaysia and Indonesia, 1 500 000 km^2). We also consider two U.S. National Parks, Cuyahoga in Ohio (130 km^2) and Rocky Mountain in Colorado (1100 km^2), where elevated Nr deposition is of concern.[26] Cuyahoga is located in the vicinity of large anthropogenic sources of Nr, while Rocky Mountain is more remote but highly sensitive to Nr deposition enrichments.[27,28]

METHOD

We use the adjoint of the GEOS-Chem CTM, a community open-source model v8.2.1 (www.geos-chem.org[29]). We focus our analysis on 2006, for which Zhang et al.[12] previously reported a detailed analysis of GEOS-Chem Nr deposition in North America including extensive comparison to observations. GEOS-Chem is driven by GEOS-5 assimilated meteorological data from the NASA Goddard Earth Observing System with horizontal resolution of 0.5° × 0.67° and 72 vertical levels. We degrade the horizontal resolution to 4° × 5° for use in GEOS-Chem. Anthropogenic emissions of NO_x and SO_2 are from the EDGAR inventory[30] and NH_3 emissions are from the GEIA inventory.[31] These global inventories are superseded by regional inventories for the U.S. (EPA NEI05), Europe (EMEP[32]), East Asia,[33] Canada (CAC[34]), and Mexico (BRAVO[35]). NO_x is also emitted from biomass burning (GFED2[36]), soil,[37,38] and lightning.[39] Anthropogenic emissions of NH_3 have seasonal variations in the U.S.,[12] Europe,[40] and Asia.[41] Natural emissions of NH_3 follow the GEIA inventory

and include emissions from soil, vegetation, and oceans.[31] Table 1 summarizes the global emissions of Nr in the model. Biogenic VOC emissions are from MEGAN v2.0.[42]

Table 1. Global Sources of Reactive Nitrogen in GEOS-Chem (2006)

source type		Tg N a^{-1}
NO_x	fuel combustion	27.8
	fossil fuel (surface)	25.7
	biofuel	1.6
	jet fuel	0.5
	soil	6.9
	open fires	5.1
	lightning	2.3
	fertilizer	0.6
	total	42.7
NH_3	agriculture	36
	natural[a]	14.3
	open fires	5.3
	biofuel	1.6
	total	57.2

[a]Ocean, soil, and excreta from wild animals.

Dry deposition is calculated using a standard resistance-in-series model[38,43] applied to a surface-type database from Olson[44] that includes local information for the receptor regions of interest. Annual mean daytime dry deposition velocities in the contiguous U.S. in GEOS-Chem are 2.7 cm s^{-1} for gaseous HNO_3, 0.65 cm s^{-1} for NH_3, and 0.15 cm s^{-1} for aerosol NH_4^+ and NO_3^-.[12] Wet deposition is treated as described by Liu et al.[45] for aerosols and by Mari et al.[46] for gases. Deposition is treated independently of emission, assuming that atmospheric and surface reservoirs are not locally coupled. Accounting for this local coupling with a surface reservoir linked to the atmospheric model[47] would extend the spatial range of

influence of sources through the re-emission process (grass-hopper effect).

The model chemistry of $NO_y \equiv NO_x + NO_3 + 2N_2O_5 + HONO + HO_2NO_2 +$ organic nitrates is based on Horowitz et al.[48] with updates summarized by Zhang et al.[12] PAN, higher peroxyacylnitrates, and alkyl nitrates are treated explicitly. Following Paulot et al.,[20] we assume that isoprene nitrates are rapidly oxidized, behaving like a temporary NO_x reservoir rather than a sink. Formation of sulfate−nitrate−ammonium aerosol is simulated with the RPMARES thermodynamic equilibrium model.[49] The model also includes heterogeneous uptake on aerosols of N_2O_5 ($N_2O_5 \rightarrow 2HNO_3$ [50]), NO_2 ($2NO_2 \rightarrow HONO + HNO_3$, $\gamma = 10^{-4}$ [51]), and NO_3 ($NO_3 \rightarrow HNO_3$, $\gamma = 10^{-3}$ [51]).

Table 2 compares the GEOS-Chem Nr deposition fluxes for the selected receptor regions to those from the TM3 CTM[25]

Table 2. Annual Nr Deposition (kg N ha^{-1} a^{-1}) in Receptor Regions[a]

	models		
receptor region	GEOS-Chem (this work)	TM3[b]	observations
Northern Hemisphere			
Cuyahoga NP	15.9		
wet NH_4^+	3.2		3.2[c]
wet NO_3^-	3.2		2.8[c]
Rocky Mountain NP	3.6		
wet NH_4^+	0.6		1.0[d]
wet NO_3^-	0.6		1.1[d]
Mesoamerica	4.4	4.5	
Southwest China	12.3	10 (10−20[e])	
Hawaii	0.8	0.5	
Southern Hemisphere			
Cerrado	4.8	6	
Madagascar	2.4	2	
Sundaland	14.2	4	
wet NH_4^+	4.5		1.5[f]
wet NO_3^-	2.9		1.4[f]

[a]Global biodiversity hotspots and U.S. National Parks (Figure 1). Values are for 2006 except TM3 (mid 1990s). [b]Phoenix et al.[25] [c]Site OH71 of the National Atmospheric Deposition Program (NADP; https://nadp.isws.illinois.edu/). [d]Site CO19 (NADP). [e]From the regional model of Lü and Tian.[57] [f]Average of sites Danum Valley and Tanah Rata of the Acid Deposition Monitoring Network in East Asia (EANET; http://www.eanet.cc/product/index.html).

and to available observations. There is generally good agreement between model and observations. The model is a factor of 2 too low at Rocky Mountain National Park but that could reflect topography not resolved on the coarse model grid scale. A nested high-resolution version of GEOS-Chem shows no such bias.[52] It is a factor of 2−3 too high in Sundaland, which suggests an overestimate of the biomass burning source. More detailed evaluations of similar GEOS-Chem versions as used here (including the same emissions) are presented by Fisher et al.[41] and Zhang et al.[12] Zhang et al.[12] conducted an extensive full-year 2006 comparison for North America with NH_x and NO_y atmospheric data and wet deposition fluxes. They found good agreement for wet deposition fluxes of NO_3^- (annual normalized mean bias (ANMB) = 8%), NH_4^+ (ANMB = 1.2%), as well as for HNO_3 (ANMB = 18%). CASTNeT calculations of HNO_3 dry deposition rates[53] are about twice

lower than GEOS-Chem but do not account for the diurnal correlation between HNO_3 concentration and dry deposition velocity and are thus likely biased low. Fisher et al.[41] compared GEOS-Chem NH_4^+ wet deposition fluxes to observations in Europe and East Asia in the spring of 2008 and found biases of less than 10%.

Figure 1 shows the simulated Nr deposition at the different receptor sites considered here. NH_x is the dominant contributor except at continental U.S. sites. Total Nr deposition is highest at Cuyahoga and Southwest China, reflecting large anthropogenic sources, and at Sundaland, reflecting large fires in Indonesia during a moderate El Niño.[54] Tropical sites show little seasonality (except for biomass burning) as dry deposition compensates for the low wet deposition during the dry season. Overall the wet contribution to total deposition is about 50%. The contribution of wet deposition to Nr deposition shows a strong seasonal cycle at tropical sites (Madagascar, Cerrado, and Mesoamerica), with a well-defined minimum during the dry season (20% in Cerrado). In Hawaii, wet deposition accounts for ~80% of Nr deposition throughout the year.

The model adjoint provides a computationally efficient way to derive the sensitivity of a given model variable (here the Nr total deposition flux) to a large ensemble of model parameters (here emissions and reaction rate constants). Briefly, at every time step we can write $c_n = F(c_{n-1})$, where c_n is a vector describing the concentration of the different chemical species simulated by the GEOS-Chem at time step n and F is the GEOS-Chem operator. If a response metric J is a function of c_n, such as total deposition flux, it can be shown using the chain rule that the gradient of J with respect to the model parameters p is given by $\nabla_p J = \sum_{i=1}^{n} ((\partial c_i)/(\partial p))^T \nabla_c J$ where $\nabla_c J = \prod_{j=1}^{n-1} ((\partial c_{j+1})/(\partial c_j))^T ((\partial J)/(\partial c_n))^T$. In the adjoint model this product is evaluated from right to left, by propagating model sensitivities backward in time. In this manner, the ensemble of model sensitivities of a model response to a large number of parameters p can be obtained by a single execution of the adjoint model. The adjoint of GEOS-Chem has been described before[55] and applied previously to diagnose the sensitivity of model concentrations to sources.[17,56] As part of this work, we constructed the adjoint component relating deposition flux to local concentrations $((\partial J)/(\partial c_n))^T$ in the above equation).

Adjoint simulations are conducted here for each receptor site of Figure 1 with J defined as the total Nr deposition in the receptor site. We explore seasonal differences in the factors driving Nr deposition (Figure 1) by applying the adjoint analysis to the months of January and July 2006 for the northern hemisphere regions and to the months of April and October 2006 for the southern tropical regions. The receptor variable is the total Nr deposition to the region for that month and the model parameter sensitivity variables are the mean values for that month and the preceding month. We calculate the sensitivity of Nr deposition to the grid-resolved emissions of NO_x and NH_3 from each source type as well as to non-Nr emissions (VOCs and SO_2) and chemical rate constants. Similar to Paulot et al.,[20] we report the sensitivity of J to processes occurring in the months under consideration and in that preceding it. In the interest of readability, we will refer to the sensitivity of Nr deposition to a specific Nr source as the "contribution" from that source. We find that the sum of adjoint sensitivities to Nr emissions closely matches total Nr deposition (Supporting Information, Figure S1), implying that the relationship between Nr sources and deposition is indeed

close to linear. Greater nonlinearity is to be expected in the relationship of Nr deposition to non-Nr emissions. Our results are for a single year (2006). Previous work for North America shows little interannual variability of Nr deposition in GEOS-Chem,[12] although larger variability would be expected in the tropics from biomass burning. In particular, 2006 biomass burning emissions in Southeast Asia (affecting Sundaland) were anomalously high.[54]

■ RESULTS AND DISCUSSION

Source Attribution. Figure 2 shows the spatial footprint of the anthropogenic Nr sources (fuel combustion and
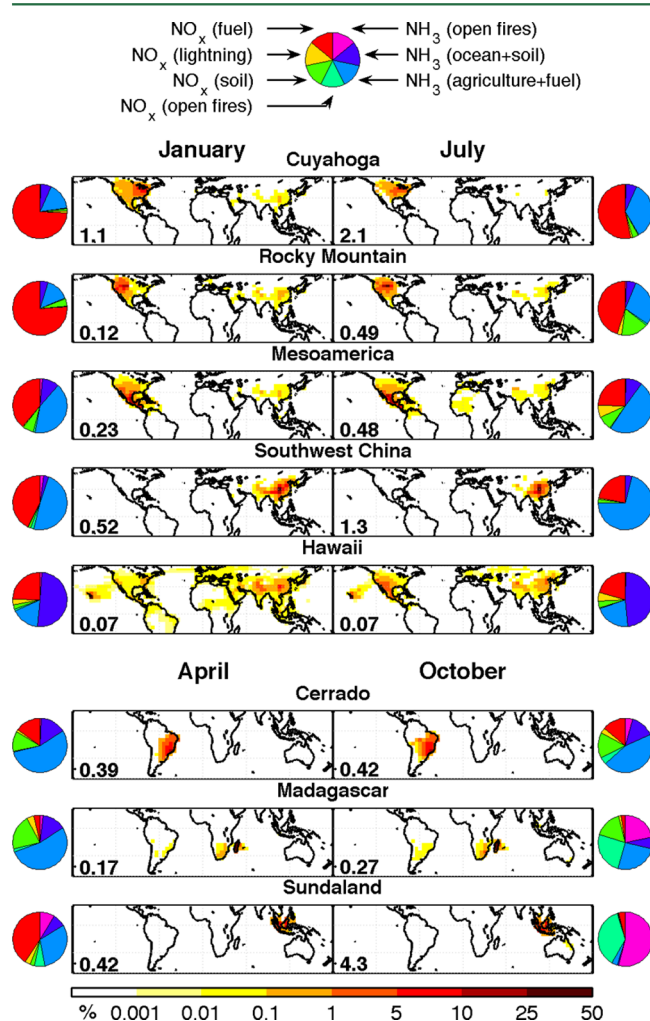

Figure 2. Source contributions to nitrogen deposition for the different receptor regions of Figure 1. The maps show the anthropogenic footprints as the fractional contribution of anthropogenic Nr emissions in each $4° × 5°$ grid cell to the anthropogenic Nr deposition (in %) in the receptor regions. The sum of all the contributions amounts to 99% of the anthropogenic component of Nr deposition. Pie charts indicate the relative contribution of different Nr source types to the total Nr deposition. The total monthly Nr deposition flux for the region (in kg N ha^{-1} month^{-1}) is shown in inset.

agriculture) contributing to Nr deposition (map) as well as the contribution from the different Nr sources (pie charts). The contribution of natural emissions to Nr deposition can be further separated into a local component, where Nr is simply recycled within the ecosystem, and an external component, where Nr is transferred between ecosystems or generated by

lightning. For our purpose we define the local component as that originating from the same $4° × 5°$ grid squares as the receptor region. Only in Hawaii and Sundaland are natural external Nr sources comparable to or greater than anthropogenic inputs. Soil NO$_x$ generally provides 10%−25% of the external natural Nr input with maximum contribution in Rocky Mountain (50%) and negligible contribution in Hawaii. Lightning NO$_x$ provides over 50% of the external natural Nr input at tropical/subtropical sites but less than 10% at midlatitude sites. The biomass burning contribution is small except in Sundaland (90%). In Hawaii, oceanic emissions of NH$_3$ account for over 85% of the natural Nr input but this source is very uncertain. Considering that Hawaiian ecosystems can be Nr-limited,[58] there is a need to better understand this oceanic source. In the following, we focus on the footprint of the anthropogenic perturbation to Nr deposition.

Anthropogenic contribution to Nr deposition ranges from 40% (Hawaii) to over 90% (Southwest China), highlighting the anthropogenic perturbation to the nitrogen cycle worldwide. Sundaland during the biomass burning season is an exception with anthropogenic sources accounting for less than 10% of Nr deposition. Most of the Nr deposition to the continental receptor regions originates from sources within that region or nearby (500 km footprint). The footprint extends further in winter at Cuyahoga and Rocky Mountain because of slower oxidation of NO$_x$ to HNO$_3$. The US account for 30−40% of the anthropogenic NO$_y$ deposited in Mesoamerica, and India accounts for 7−13% of the anthropogenic Nr deposited in Southwest China.

Intercontinental transport makes little contribution to Nr deposition except at Hawaii, consistent with the previous model study by Sanderson et al.[13] For example, Asian anthropogenic sources account for only 7% of NH$_x$ deposition at Rocky Mountain and 3% at Cuyahoga. At Hawaii, however, trans-pacific transport accounts for ∼40% of the anthropogenic Nr deposition, with a marked seasonal shift between winter and summer sources that reflects changes in the position of the North Pacific anticyclone.[59] In winter, sources are dominated by Asia with China and India contributing, respectively, 19% and 10% of the anthropogenic Nr. In contrast, in summer, the U.S. and Mexico together contribute ∼30% of the anthropogenic Nr deposition.

Sensitivity to Non-Nr Sources. SO$_2$ emissions affect the deposition of Nr through the formation of sulfate−nitrate−ammonium aerosol, changing the partitioning of Nr between the gas and particle phases. Figure 3 shows the sensitivity of Nr deposition to SO$_2$ emissions (blue bars) relative to NH$_3$ emission. The effect can be large, up to 30% at Cuyahoga in winter, and variable in sign. Greater SO$_2$ emissions increase the fraction of NH$_x$ in the particle phase as ammonium, which generally lengthens the NH$_x$ lifetime as particles are more resistant to dry deposition. Thus sources of SO$_2$ located outside of receptor regions generally increase Nr deposition in these regions (e.g., SO$_2$ sources in the U.S. for summertime Mesoamerica), while SO$_2$ emissions located within the receptor region tend to favor Nr export (e.g., wintertime Mesoamerica). However, increasing SO$_2$ emissions can also promote the volatilization of nitrate, particularly in winter, and hence increase its local deposition as HNO$_3$ as gaseous HNO$_3$ deposits faster than particulate nitrate.[12] This explains the large positive sensitivity at Cuyahoga during that season.

Figure 3 also shows the response of Nr deposition to increasing emissions of anthropogenic VOCs (AVOCs, red)
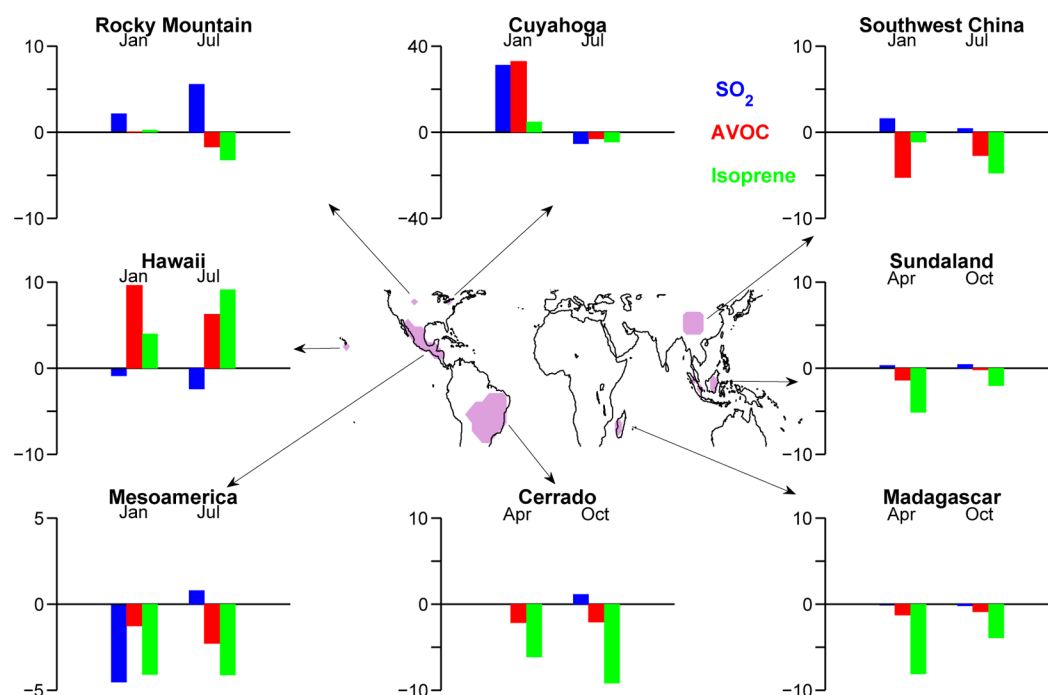
Figure 3. Sensitivity of Nr deposition to global non-Nr emissions, expressed as percentages of the sensitivity to NH_3 emissions (for SO_2 (blue)) and of the sensitivity to NO_x emissions (for anthropogenic VOCs (AVOCs, red) and isoprene (green)) in January/April and July/October at northern/southern hemisphere sites. Note the difference in scales among panels.

and biogenic isoprene (green). VOCs affect Nr deposition by changing OH and ozone concentrations (thus changing the lifetime of NO_x against oxidation to HNO_3) and by converting NO_x to organic nitrates that do not deposit as readily as HNO_3. The transport of these organic nitrates and the subsequent release of NO_x far from its point of origin[9] causes the positive response of Nr deposition in Hawaii to global VOC emissions. In contrast, in low-NO_x regions such as Cerrado, OH depletion by isoprene photooxidation slows down the oxidation of NO_x to nitric acid and enables the conversion of a large fraction of NO_x to isoprene nitrates,[20] causing a large negative sensitivity of Nr deposition to isoprene emission.

We see from the above discussion that the sensitivity of Nr deposition to SO_2 or VOC emissions can change sign depending on the chemical environment and the distance of these emissions from the receptor region. Thus, the spatially integrated sensitivities shown in Figure 3 often reflect some cancellation between positive and negative regional dependences. This is illustrated in Figure 4 with the sensitivity of NO_y deposition to spatially resolved isoprene emissions at Cuyahoga (circle) in summer. Emissions of isoprene in the Northeast U.S., close to Cuyahoga, inhibit NO_y deposition while large upwind emissions in the U.S. Southeast increase it.

The large positive sensitivity of NO_y deposition to AVOC emissions at Cuyahoga in winter (Figure 3) reflects the importance of AVOCs in driving ozone production under NO_x-saturated conditions,[60] in turn promoting NO_3 formation from the reaction of NO_2 with ozone. This favors the production of N_2O_5, hydrolysis of which is the primary source of HNO_3 in winter midlatitudes.[61] Such polluted wintertime conditions also cause Nr deposition to depend on chemical rate constants in nonobvious ways. The sensitivity to the N_2O_5 reactive uptake probability ($\gamma_{N_2O_5}$) is small (<1% of the sensitivity to NO_x emissions) because its formation is limited by NO_3. We find that a decrease in the reaction rate coefficient for OH + NO_2[62]
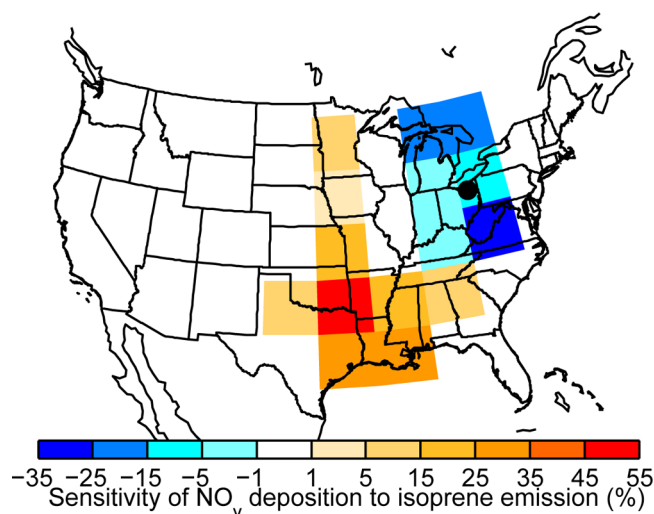

Figure 4. Sensitivity of NO_y deposition in July at Cuyahoga National Park (black circle) to spatially resolved isoprene emissions. The grid-resolved sensitivity to isoprene emissions is divided by the sensitivity to collocated NO_x emissions. The sum of the absolute individual sensitivities shown here amounts to 90% of the overall absolute sensitivity of Nr deposition to isoprene emissions (see Figure 3).

would increase Nr deposition (~−45% of the sensitivity to NO_x emissions). Though OH + NO_2 is a source of nitric acid, it is also a sink of hydrogen oxide radicals (HO_x) and thus limits ozone production. We also find a large positive sensitivity (~40% of the sensitivity to NO_x emissions) to the reactive uptake probability of NO_2 on aerosols ($2NO_2 \rightarrow HONO + HNO_3$). The most important impact of this reaction on Nr deposition is indirect: it contributes ~45% of HO_x production at Cuyahoga in the wintertime and thus promotes the production of N_2O_5. Recent laboratory studies[63−66] suggest
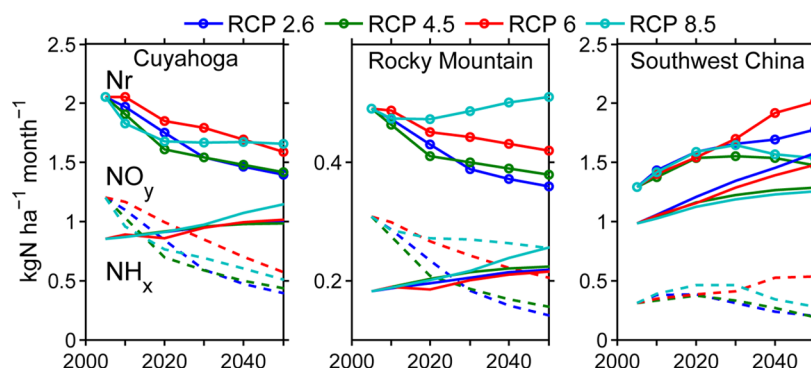
Figure 5. Future Nr deposition in July under the four Representative Concentration Pathways (RCP) scenarios[69] adopted by the IPCC. For each scenario, the deposition of total Nr (solid line with circles), NO_y (dash line), and NH_x (solid line) are calculated by multiplying gridded changes in Nr emissions by the corresponding adjoint sensitivities.

that the NO_2 reactive uptake probability of 10^{-4} used in GEOS-Chem may be more than 1 order of magnitude too high. Uncertainty in the wintertime sources of HONO[67] could contribute to the overestimate of nitrate deposition and concentration in GEOS-Chem.[12,68]

Future Projections. The Intergovernmental Panel on Climate Change (IPCC) has recently adopted four global gridded emission projections for the 21st century as Representative Concentration Pathways (RCPs) designed to achieve a certain radiative forcing cap by 2100.[69] The RCP scenarios are defined by the magnitude of this cap (for example, RCP2.6 assumes a cap of 2.6 W m^{-2}). In these scenarios, future NO_x emissions decrease in response to stringent emission controls in the U.S. and Europe,[70,71] while NH_3 emissions continue to increase because of the world's growing demand for food (Supporting Information, Figure S1). The source–receptor relationships calculated from the adjoint model allow us to readily estimate the response of Nr deposition to these or other emission projections, assuming that the response is linear and time-invariant and that the meteorology does not change. We find in our work that the sum of adjoint sensitivities to Nr emissions closely matches total Nr deposition (Supporting Information, Table S1), implying that the relationship between Nr sources and deposition is indeed close to linear.

Figure 5 shows the projected changes in Nr deposition out to 2050 for Cuyahoga, Rocky Mountain, and Southwest China for the four RCP scenarios. Nr deposition in Southwest China is expected to increase by ~20% in the next decade in all scenarios. In the 2020s, Nr deposition decreases in the RCP4.5 and RCP8.5 scenarios reflecting the widespread adoption of air pollution regulations. However, in the RCP6 scenario, delayed regulation of industrial emissions results in an increase of Nr deposition by ~75% by 2050. Nr deposition is expected to decrease at the U.S. sites except in the RCP8.5 scenario, consistent with the results of Lamarque et al.[72] due to lower NO_x emissions. By 2030, in all scenarios, NH_x is predicted to be the largest contributor to Nr deposition at Cuyahoga. As a result, Nr deposition improves much less after 2025. At the Rocky Mountain site, increasing NH_3 emissions result in increasing Nr deposition in the RCP8.5 scenario. For both national parks, Nr deposition will continue to exceed the ecoregion critical load (3−8 kg N ha^{-1} a^{-1} at Cuyahoga ; 3 kg N ha^{-1} a^{-1} at Rocky Mountain[73]) in the coming decades. Decrease of agricultural NH_3 emissions will become necessary after 2020 to significantly diminish Nr deposition.

■ ASSOCIATED CONTENT

ⓢ Supporting Information

Evaluation of the linearity of Nr deposition and trends in RCP emissions of NO, NH_3, and Nr in the U.S. and China. This material is available free of charge via the Internet at http://pubs.acs.org.

■ AUTHOR INFORMATION

Corresponding Author
*E-mail: paulot@seas.harvard.edu.

Notes
The authors declare no competing financial interest.

■ ACKNOWLEDGMENTS

■ REFERENCES

(1) Galloway, J. N.; Dentener, F. J.; Capone, D. G.; Boyer, E. W.; Howarth, R. W.; Seitzinger, S. P.; Asner, G. P.; Cleveland, C. C.; Green, P. A.; Holland, E. A.; Karl, D. M.; Michaels, A. F.; Porter, J. H.; Townsend, A. R.; Vöosmarty, C. J. Nitrogen cycles: past, present, and future. *Biogeochemistry* **2004**, *70*, 153−226.

(2) Magnani, F.; et al. The human footprint in the carbon cycle of temperate and boreal forests. *Nature* **2007**, *447*, 849−851.

(3) Pregitzer, K. S.; Burton, A. J.; Zak, D. R.; Talhelm, A. F. Simulated chronic nitrogen deposition increases carbon storage in Northern Temperate forests. *Global Change Biol.* **2008**, *14*, 142−153.

(4) Reay, D. S.; Dentener, F.; Smith, P.; Grace, J.; Feely, R. A. Global nitrogen deposition and carbon sinks. *Nat. Geosci.* **2008**, *1*, 430−437.

(5) Sala, O. E.; et al. Global Biodiversity Scenarios for the Year 2100. *Science* **2000**, *287*, 1770−1774.

(6) Johnson, P. T. J.; Townsend, A. R.; Cleveland, C. C.; Glibert, P. M.; Howarth, R. W.; McKenzie, V. J.; Rejmankova, E.; Ward, M. H. Linking environmental nutrient enrichment and disease emergence in humans and wildlife. *Ecol. Appl.* **2010**, *20*, 16−29.

(7) Bergström, A.-K.; Jansoon, M. Atmospheric nitrogen deposition has caused nitrogen enrichment and eutrophication of lakes in the northern hemisphere. *Global Change Biol.* **2006**, *12*, 635−643.

(8) Bobbink, R.; et al. Global assessment of nitrogen deposition effects on terrestrial plant diversity: A synthesis. *Ecol. Appl.* **2010**, *20*, 30−59.

(9) Moxim, W. J.; Levy, I., H.; Kasibhatla, P. S. Simulated global tropospheric PAN: Its transport and impact on NO_x. *J. Geophys. Res.* **1996**, *101*, 12621−12638.

(10) Atherton, C. S. Organic nitrates in remote marine environments: Evidence for long range transport. *Geophys. Res. Lett.* **1989**, *16*, 1289−1292.

(11) Dentener, F.; et al. Nitrogen and sulfur deposition on regional and global scales: A multimodel evaluation. *Global Biogeochem. Cycles* **2006**, *20*, B4003.

(12) Zhang, L.; Jacob, D. J.; Knipping, E. M.; Kumar, N.; Munger, J. W.; Carouge, C. C.; van Donkelaar, A.; Wang, Y. X.; Chen, D. Nitrogen deposition to the United States: Distribution, sources, and processes. *Atmos. Chem. Phys.* **2012**, *12*, 4539−4554.

(13) Sanderson, M. G.; et al. A multi-model study of the hemispheric transport and deposition of oxidised nitrogen. *Geophys. Res. Lett.* **2008**, *35*, L17815.

(14) Giering, R.; Kaminski, T. Recipes for adjoint code construction. *ACM T. Math. Software* **1998**, *24*, 437−474.

(15) Errico, R. M. What is an adjoint model? *Bull. Am. Meteorol. Soc.* **1997**, *78*, 2577−2591.

(16) Vukićević, T.; Hess, P. Analysis of tropospheric transport in the Pacific Basin using the adjoint technique. *J. Geophys. Res.* **2000**, *105*, 7213−7230.

(17) Zhang, L.; Jacob, D. J.; Kopacz, M.; Henze, D. K.; Singh, K.; Jaffe, D. A. Intercontinental source attribution of ozone pollution at western U.S. sites using an adjoint method. *Geophys. Res. Lett.* **2009**, *36*, L11810.

(18) Menut, L.; Vautard, R.; Beekmann, M.; Honoré, C. Sensitivity of photochemical pollution using the adjoint of a simplified chemistry-transport model. *J. Geophys. Res.* **2000**, *105*, 15379−15402.

(19) Vautard, R.; Beekmann, M.; Menut, L. Applications of adjoint modelling in atmospheric chemistry: Sensitivity and inverse modelling. *Environ. Modell. Softw.* **2000**, *15*, 703−709.

(20) Paulot, F.; Henze, D. K.; Wennberg, P. O. Impact of the isoprene photochemical cascade on tropical ozone. *Atmos. Chem. Phys.* **2012**, *12*, 1307−1325.

(21) Walker, T. W.; et al. Impacts of midlatitude precursor emissions and local photochemistry on ozone abundances in the Arctic. *J. Geophys. Res.* **2012**, *117*, D01305.

(22) Kopacz, M.; Mauzerall, D. L.; Wang, J.; Leibensperger, E. M.; Henze, D. K.; Singh, K. Origin and radiative forcing of black carbon transported to the Himalayas and Tibetan Plateau. *Atmos. Chem. Phys.* **2011**, *11*, 2837−2852.

(23) Myers, N.; Mittermeier, R. A.; Mittermeier, C. G.; da Fonseca, G. A. B.; Kent, J. Biodiversity hotspots for conservation priorities. *Nature* **2000**, *403*, 853−858.

(24) Conservation International. *The Biodiversity Hotspots.* http://www.conservation.org/where/priority_areas/hotspots/Pages/hotspots_main.aspx

(25) Phoenix, G. K.; Hicks, W. K.; Cinderby, S.; Kuylenstierna, J. C. I.; Stock, W. D.; Dentener, F. J.; Giller, K. E.; Austin, A. T.; Lefroy, R. D. B.; Gimeno, B. S.; Ashmore, M. R.; Ineson, P. Atmospheric nitrogen deposition in world biodiversity hotspots: The need for a greater global perspective in assessing N deposition impacts. *Global Change Biol.* **2006**, *12*, 470−476.

(26) Sullivan, T. J.; McDonnell, T. C.; McPherson, G. T.; Mackey, S. D.;Moore, D. *Evaluation of the Sensitivity of Inventory and Monitoring National Parks to Nutrient Enrichment Effects from Atmospheric Nitrogen Deposition*; Natural Resource Report NPS/NRPC/ARD/NRR−2011/313; U.S. National Park Service, 2011.

(27) Wolfe, A. P.; Van Gorp, A. C.; Baron, J. S. Recent ecological and biogeochemical changes in alpine lakes of Rocky Mountain National Park (Colorado, USA): A response to anthropogenic nitrogen deposition. *Geobiology* **2003**, *1*, 153−168.

(28) Baron, J. S.; Rueth, H. M.; Wolfe, A. M.; Nydick, K. R.; Allstott, E. J.; Minear, J. T.; Moraska, B. Ecosystem Responses to Nitrogen Deposition in the Colorado Front Range. *Ecosystems* **2000**, *3*, 352−368, DOI: 10.1007/s100210000032.

(29) Bey, I.; Jacob, D. J.; Yantosca, R. M.; Logan, J. A.; Field, B. D.; Fiore, A. M.; Li, Q.; Liu, H. Y.; Mickley, L. J.; Schultz, M. G. Global modeling of tropospheric chemistry with assimilated meteorology −

Model description and evaluation. *J. Geophys. Res.* **2001**, *106*, 23073−23095.

(30) Olivier, J. G. J.; Berdowski, J. J. M. Global emission sources and sinks. In *The Climate System*; Berdowski, J., GuicheritR., Heij, B. J., Eds.; A.A. Balkema Publishers/Swets & Zeitlinger Publishers: Lisse, The Netherlands, 2001; pp 33−77

(31) Bouwman, A. F.; Lee, D. S.; Asman, W. A. H.; Dentener, F. J.; Van Der Hoek, K. W.; Olivier, J. G. J. A global high-resolution emission inventory for ammonia. *Global Biogeochem. Cycles* **1997**, *11*, 561−587.

(32) Vestreng, V.; Klein, H. *Emission data reported to UNECE/EMEP: Quality assurance and trend analysis & Presentation of WebDab*; Norwegian Meteorological Institute, 2002.

(33) Streets, D. G.; Bond, T. C.; Carmichael, G. R.; Fernandes, S. D.; Fu, Q.; He, D.; Klimont, Z.; Nelson, S. M.; Tsai, N. Y.; Wang, M. Q.; Woo, J.; Yarber, K. F. An inventory of gaseous and primary aerosol emissions in Asia in the year 2000. *J. Geophys. Res.* **2003**, *108*, 8809.

(34) Environment Canada. *National Pollutant Release Inventory.* http://www.ec.gc.ca/pdb/cac/cachomee.cfm

(35) Kuhns, H.; Knipping, E.; Vukovich, J. Development of a United States-Mexico Emissions inventory for the big bend regional aerosol and visibility observational (BRAVO) study. *J. Air Waste Manage.* **2005**, *55*, 677−692.

(36) Randerson, J. T.; van der Werf, G. R.; Giglio, L.; Collatz, G. J.; Kasibhatla, P. S. *Global Fire Emissions Database*, Version 2 (GFEDv2); 2006.

(37) Yienger, J. J.; Levy, H. Empirical model of global soil-biogenic NO_x emissions. *J. Geophys. Res.* **1995**, *100*, 11447−11464.

(38) Wang, Y.; Jacob, D. J.; Logan, J. A. Global simulation of tropospheric O_3-NO_x-hydrocarbon chemistry 1. Model formulation. *J. Geophys. Res.* **1998**, *103*, 10713−10726.

(39) Sauvage, B.; Martin, R. V.; van Donkelaar, A.; Liu, X.; Chance, K.; Jaeglé, L.; Palmer, P. I.; Wu, S.; Fu, T.-M. Remote sensed and in situ constraints on processes affecting tropical tropospheric ozone. *Atmos. Chem. Phys.* **2007**, *7*, 815−838.

(40) Friedrich, R.; Reis, S. In *Emissions of Air Pollutants - Measurements, Calculations and Uncertainties.*; Friedrich, R., Reis, S., Eds.; Springer-Verlag, 2004.

(41) Fisher, J. A.; et al. Sources, distribution, and acidity of sulfate-ammonium aerosol in the Arctic in winter-spring. *Atmos. Environ.* **2011**, *45*, 7301−7318.

(42) Guenther, A.; Karl, T.; Harley, P.; Wiedinmyer, C.; Palmer, P. I.; Geron, C. Estimates of global terrestrial isoprene emissions using MEGAN (Model of Emissions of Gases and Aerosols from Nature). *Atmos. Chem. Phys.* **2006**, *6*, 3181−3210.

(43) Wesely, M. . L. Parameterization of surface resistances to gaseous dry deposition in regional-scale numerical models. *Atmos. Environ.* **1989**, *23*, 1293−1304.

(44) Olson, J. *World Ecosystems (WE1.4): Digital raster data on a 10 minute geographic 1080 x 2160 grid*; 1992.

(45) Liu, H.; Jacob, D. J.; Bey, I.; Yantosca, R. M. Constraints from ^{210}Pb and ^7Be on wet deposition and transport in a global three-dimensional chemical tracer model driven by assimilated meteorological fields. *J. Geophys. Res.* **2001**, *106*, 12109−12128.

(46) Mari, C.; Bechtold, P.; Jacob, D. Transport and scavenging of soluble gases in a deep convective cloud. *J. Geophys. Res.* **2000**, *105*, 22255−22268.

(47) Cooter, E. J.; Bash, J. O.; Walker, J. T.; Jones, M.; Robarge, W. Estimation of NH_3 bi-directional flux from managed agricultural soils. *Atmos. Environ.* **2010**, *44*, 2107−2115.

(48) Horowitz, L. W.; Liang, J.; Gardner, G. M.; Jacob, D. J. Export of reactive nitrogen from North America during summertime — Sensitivity to hydrocarbon chemistry. *J. Geophys. Res.* **1998**, *103*, 13451−13476.

(49) Binkowski, F. S.; Roselle, S. J. Models-3 Community Multiscale Air Quality (CMAQ) model aerosol component 1. Model description. *J. Geophys. Res.* **2003**, *108*.

(50) Evans, M. J.; Jacob, D. Impact of new laboratory studies of N_2O_5 hydrolysis on global model budgets of tropospheric nitrogen oxides, ozone, and OH. *Geophys. Res. Lett.* **2005**, *32*, 1−4.

(51) Jacob, D. J. Heterogeneous chemistry and tropospheric ozone. *Atmos. Environ.* **2000**, *34*, 2131−2159.

(52) Ellis, R. A.; Jacob, D. J.; Payer, M.; Zhang, L.; Holmes, C. D.; Schichtel, B. A.; Blett, T.; Porter, E.; Pardo, L. H.; Lynch, J. A. Present and Future Nitrogen Deposition to National Parks in the United States: Critical Load Exceedances. *Atmos. Chem. Phys. Discuss.* **2013**, submitted.

(53) Clarke, J.; Edgerton, E.; Martin, B. Dry deposition calculations for the clean air status and trends network. *Atmos. Environ.* **1997**, *31*, 3667−3678.

(54) Logan, J. A.; Megretskaia, I.; Nassar, R.; Murray, L. T.; Zhang, L.; Bowman, K. W.; Worden, H. M.; Luo, M. Effects of the 2006 El Nino on tropospheric composition as revealed by data from the Tropospheric Emission Spectrometer (TES). *Geophys. Res. Lett.* **2008**, *35*, L03816

(55) Henze, D. K.; Seinfeld, J. H.; Shindell, D. T. Inverse modeling and mapping US air quality influences of inorganic $PM_{2.5}$ precursor emissions using the adjoint of GEOS-Chem. *Atmos. Chem. Phys.* **2009**, *9*, 5877−5903.

(56) Kopacz, M.; Mauzerall, D. L.; Wang, J.; Leibensperger, E. M.; Henze, D. K.; Singh, K. Origin and radiative forcing of black carbon transported to the Himalayas and Tibetan Plateau. *Atmos. Chem. Phys.* **2011**, *11*, 2837−2852.

(57) Lü, C.; Tian, H. Spatial and temporal patterns of nitrogen deposition in China: Synthesis of observational data. *J. Geophys. Res.* **2007**, *112*

(58) Vitousek, P. M.; Walker, L. R.; Whiteaker, L. D.; Matson, P. A. Nutrient limitations to plant growth during primary succession in Hawaii Volcanoes National Park. *Biogeochemistry* **1993**, *23*, 197−215, DOI: 10.1007/BF00023752.

(59) Moxim, W. J. Simulated Transport of NO_y to Hawaii During August: A Synoptic Study. *J. Geophys. Res.* **1990**, *95*, 5717−5729.

(60) Jacob, D.; Horowitz, L.; Munger, J.; Heikes, B.; Dickerson, R.; Artz, R.; Keene, W. Seasonal transition from NO_x-to hydrocarbon-limited conditions for ozone production over the eastern United States in September. *J. Geophys. Res.* **1995**, *100*, 9315−9324.

(61) Dentener, F. J.; Crutzen, P. J. Reaction of N_2O_5 on Tropospheric Aerosols: Impact on the Global Distributions of NO_x, O_3, and OH. *J. Geophys. Res.* **1993**, *98*, 7149−7163.

(62) Mollner, A. K.; Valluvadasan, S.; Feng, L.; Sprague, M. K.; Okumura, M.; Milligan, D. B.; Bloss, W. J.; Sander, S. P.; Martien, P. T.; Harley, R. A.; McCoy, A. B.; Carter, W. P. L. Rate of Gas Phase Association of Hydroxyl Radical and Nitrogen Dioxide. *Science* **2010**, *330*, 646−649.

(63) Kleffmann, J.; Becker, K.; Wiesen, P. Heterogeneous NO_2 conversion processes on acid surfaces: Possible atmospheric implications. *Atmos. Environ.* **1998**, *32*, 2721−2729.

(64) Cheung, J. L.; Li, Y. Q.; Boniface, J.; Shi, Q.; Davidovits, P.; Worsnop, D. R.; Jayne, J. T.; Kolb, C. E. Heterogeneous Interactions of NO_2 with Aqueous Surfaces. *J. Phys. Chem. A* **2000**, *104*, 2655−2662.

(65) Kurtenbach, R.; Becker, K.; Gomes, J.; Kleffmann, J.; Lörzer, J.; Spittler, M.; Wiesen, P.; Ackermann, R.; Geyer, A.; Platt, U. Investigations of emissions and heterogeneous formation of HONO in a road traffic tunnel. *Atmos. Environ.* **2001**, *35*, 3385−3394.

(66) Finlayson-Pitts, B. J.; Wingen, L. M.; Sumner, A. L.; Syomin, D.; Ramazan, K. A. The heterogeneous hydrolysis of NO_2 in laboratory systems and in outdoor and indoor atmospheres: An integrated mechanism. *Phys. Chem. Chem. Phys.* **2003**, *5*, 223−242.

(67) Elshorbany, Y. F.; Steil, B.; Brühl, C.; Lelieveld, J. Impact of HONO on global atmospheric chemistry calculated with an empirical parameterization in the EMAC model. *Atmos. Chem. Phys.* **2012**, *12*, 9977−10000.

(68) Heald, C. L.; Collett, J. L.; Lee, T.; Benedict, K. B.; Schwandner, F. M.; Li, Y.; Clarisse, L.; Hurtmans, D. R.; Van Damme, M.; Clerbaux, C.; Coheur, P.-F.; Pye, H. O. T. Atmospheric ammonia and particulate inorganic nitrogen over the United States. *Atmos. Chem. Phys.* **2012**, *12*, 10295−10312.

(69) van Vuuren, D.; Edmonds, J.; Kainuma, M.; Riahi, K.; Thomson, A.; Hibbard, K.; Hurtt, G.; Kram, T.; Krey, V.; Lamarque, J.-F.; Masui, T.; Meinshausen, M.; Nakicenovic, N.; Smith, S.; Rose, S. The representative concentration pathways: An overview. *Clim. Change* **2011**, *109*, 5−31, DOI: 10.1007/s10584-011-0148-z.

(70) Kim, S. W.; Heckel, A.; McKeen, S. A.; Frost, G. J.; Hsie, E. Y.; Trainer, M. K.; Richter, A.; Burrows, J. P.; Peckham, S. E.; Grell, G. A. Satellite-observed U.S. power plant NO_x emission reductions and their impact on air quality. *Geophys. Res. Lett.* **2006**, *33*, L22812.

(71) van der A, R. J.; Eskes, H. J.; Boersma, K. F.; van Noije, T. P. C.; Van Roozendael, M.; De Smedt, I.; Peters, D. H. M. U.; Meijer, E. W. Trends, seasonal variability and dominant NO_x source derived from a ten year record of NO_2 measured from space. *J. Geophys. Res.* **2008**, *113*, D04302.

(72) Lamarque, J.-F.; Kyle, G.; Meinshausen, M.; Riahi, K.; Smith, S.; van Vuuren, D.; Conley, A.; Vitt, F. Global and regional evolution of short-lived radiatively-active gases and aerosols in the Representative Concentration Pathways. *Clim. Change* **2011**, *109*, 191−212, DOI: 10.1007/s10584-011-0155-0.

(73) Pardo, L. H.; et al. Effects of nitrogen deposition and empirical nitrogen critical loads for ecoregions of the United States. *Ecol. Appl.* **2011**, *21*, 3049−3082.